This is to certify that the

thesis entitled
Ultrasensitive Detector System for a High Performance Hybrid Mass Spectrometer

presented by
Luis A. Romero

has been accepted towards fulfillment
of the requirements for

Master degree in Chemistry

George D. Dorsi
Major professor

Date Nov. 1, 1989

# ULTRASENSITIVE DETECTOR SYSTEM FOR A HIGH PERFORMANCE HYBRID MASS SPECTROMETER

By

Luis A. Romero

A THESIS

Submitted to
Michigan State University
in partial fulfillment of the requirements
of the degree of

MASTER OF SCIENCE

Department of Chemistry

1989

***ABSTRACT***

*by*

*Luis A. Romero*

An ion beam (double focusing) mass spectrometer coupled to a collision cell and followed by a quadrupole mass filter, is being constructed in the MSU Chemistry Department. It will be a powerful instrument that will provide experimental information concerning bond energies and threshold energies of reactions, among others (between organic molecules and atoms/ions/complexes). However, in order to perform such experiments, it is necessary to implement a detection system capable of measuring low fluxes of ions. The subject of this thesis is the design and construction of the detection system for the ion beam instrument.

The photon counting detection was chosen as the optimum method for this application. The different criteria involved in its selection are discussed. Comparison of different types of detection schemes are also included. In addition, models of different types of photon counting systems are examined using a simulation program (SIMION 4.0) which allows the relative efficiency to be determined. Design criteria and operational procedures for the detection system are described. Discussion of the

different problems encountered during the design and construction process is included, as are the different approaches taken to solve such problems. The current status of the working detector is documented and further work is recommended in order to complete the characterization process of the overall system.

**To my family and my wife**

**ACKNOWLEDGMENTS**

To those who have contributed in my personal growth and have been there in every time when their moral support was most needed.

I would also like to offer my must sincerely thanks to the following people, all of whom have made direct contributions to the development of the detector system (the subject of this thesis).

George Leroi and John Allison for their guidance, support, encouragement, advice and patience (among others) during all this time of my graduate student life. Also Paul O'Connors by all the help and information that he shared with me during all this work.

Marty Rabb, MSU Chemistry Electronic Designer for designing the pulsating circuit used as well as for all his advice in some of the electronic problems encountered during this work.

Russ Geyer, Dick Menke and Dick Watters, the staff of the MSU Chemistry Department Machine shop for their carefully machining of the vacuum chamber, enhancer dynode and other parts of the detection system.

Reg Renninger and John Yurkon from the Cyclotron Facility which provide us with the scintillator material and coated with the aluminum oxide and also provide us with enough technical information to start

developing the detector.

Finally, I would like to acknowledge the financial support provided by Michigan State University during all these years as a graduate student.

## TABLE OF CONTENTS

## LIST OF TABLES

## LIST OF FIGURES

# CHAPTER I

## INTRODUCTION

A new ion beam tandem mass spectrometer is being developed through collaboration between the Allison and Leroi research groups in the MSU Chemistry Department. The instrument will consist of: (1) single beam Varian MAT CH-5 DF double focussing mass spectrometer, (2) deceleration lens system, (3) radio frequency-only octopole ion beam guide/ collision cell, (4) quadrupole mass filter and (5) ion flux detection system. Figure 1.1 shows a schematic diagram of the instrument.

The goal in the development of this instrument is to provide insights into the nature of reactions between organic molecules and metal atoms\ions\complexes. It will also allow experimental determinations of bond energies and energetic reaction barriers and provide information about ionic structures. The apparatus is designed to allow accurate measurements of ion energies in an experimental laboratory energy range from 0.05 to 500 eV. Therefore, it requires a detection system, the topic of this thesis, capable of measuring low ion fluxes at these threshold energies.

In general, mass spectrometers require sensitive, fast-response ion detectors to measure very small currents or to record very rapidly scanned mass spectra. This can be accomplished by the use of a direct

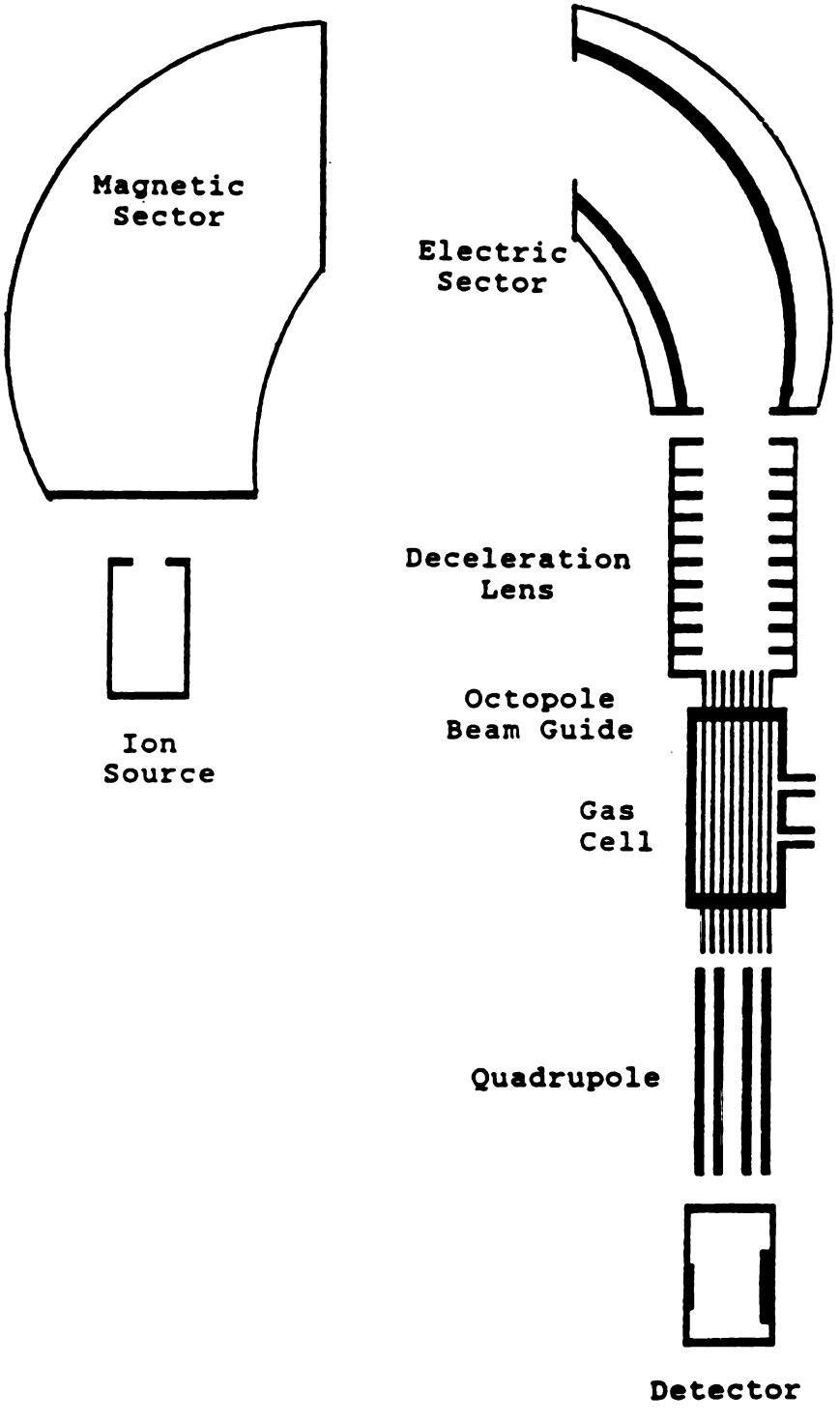


**Figure 1.1. Proposed MSU Ion Beam Instrument**

or an indirect method of detection[1,2]. Unfortunately when the direct method of detection, (e.g., Faraday cup) is employed to record relatively rapidly scanned mass spectra (less than 0.1 seconds for a mass range of 50 to 500), its sensitivity is usually low ($10^{-14}$ A).[1] With the indirect method (e.g., scintillation detection), higher sensitivity can be achieved ($10^{-20}$A),[2] even for relative rapidly scanned mass spectra (less than 0.1 s for a mass range of 50 to 500).

In order for the detection system to be useful for the chemical experiments of interest in this project, it must meet certain requirements. These requirements include: (1) high sensitivity ($10^{-20}$ A), in order to measure ion intensities at threshold energies of reactions, (2) fast response time (nanosecond range), (3) good signal-to-noise ratio, (4) short and long term linearity, for quantitative work, (5) long and short term stability, (6) long serviceable life (little deterioration over long periods of use), and (7) simplicity and cost-effectiveness. The detection method that can best meet these requirements is the indirect method of detection.

The first task undertaken in this research project was the design and construction of the detection system. The design process included a comparison between different indirect methods of detection such as electron multipliers (discrete and continuous dynode versions), and scintillator detectors. Table 1.1 presents a summary of their main

**Table 1.1**

**Ion Detector Characteristics**

| Type | Maximum Sensitivity (A) | Main Use | Advantage | Disadvantages |
|---|---|---|---|---|
| Faraday cage | $10^{-17(a)}$ | Isotopic abundance, Quantitative analysis, Research | Reliable | Poor sensitivity |
| Electron Multiplier | $10^{-20}$ | Research, Isotopic abundance | High sensitivity, Ion counting | Short life, Cost |
| Scintillator Detectors | $10^{-20}$ | Research, Isotopic abundance | High sensitivity, Ion counting, Long life | High voltage |

(a) With vibrating reed electrometer; less with other types of ammeters

characteristics.

Computerized modeling of several scintillator detection systems has been done with an ion trajectory simulation program, SIMION 4.0.[3] This is an interactive program developed for microcomputers (e.g., IBM AT/XT and Apple MACINTOSH) which allows the simulation of ion trajectories through ion optical components.

The selection as well as design considerations of the detector system will be the subject of chapter 2. Chapter 3 deals with operational procedures for the detector. Experimental results and discussion of them will be presented in chapter 4. A description of the current status of the system is given in chapter 5.

# CHAPTER 2

## Detection System Design

### 2.1 Detection System Selection Criteria

The ion beam tandem mass spectrometer under construction is designed to allow accurate measurements at threshold energies of reaction. Under such conditions the number of ions/sec that will be detected are in the range of $10^3$ to $10^1$ or fewer. This corresponds to ion currents of $10^{-16}$ to $10^{-18}$ amperes. Therefore, the most important criterion for the detection system is its sensitivity over that range. In addition, the detector should provide: (a) S/N ratios that allow the measurement of the above currents to a precision of at least ± 10%, (b) fast response time (nanosecond range), and (c) short and long term stability. The two most common methods of detection for this range are ones which utilize electron multipliers or scintillators.

### 2.2 Electron Multipliers

Electron multipliers use the principle of secondary-electron emission amplification.[1] They are classified as either discrete or continuous dynode electron multipliers. The difference between them is the way in which the secondary-electron emission surface is constructed (discrete or continuous).

Electron multipliers can amplify ion currents by factors up to $10^8$, depending on which type of multiplier is used and on its condition.[4]

The amplification factors obtainable using electron multipliers give high sensitivity to the current-measuring system. These detectors are also characterized by fast response time (nanosecond range for continuous and some discrete dynodes)[5] and good S/N ratio (± 10% for ion currents of $10^{-18}$A).[4] These properties allow the use of electron multipliers in analog as well as in pulse detection modes.

Unfortunately, electron multipliers can offer only short term stability. Degradation in performance is observed as a function of time of use. The initial gain decreases rapidly (from values of $10^6$ or higher to $10^5$) and then more slowly, progressively to lower values.[4] This can be attributed to: (1) ionization of residual gases which are normally present between dynodes and (2) the catalytic action of secondary electrons which polymerizes hydrocarbons on a dynode surface, thus lowering secondary electron yields. The rate of deterioration, therefore, depends strongly on the space current of electrons flowing through an electron multiplier and on residual gas pressure.[6]

## 2.3 Scintillator Detector Systems

Scintillator detector devices, as do electron multipliers, use the principle of secondary-electron emission amplification. In these devices a form of ionizing radiation (i.e., α-particle, ß-particle, electron, etc.) interacts with scintillator material which produces an excited electron and a low energy photon. The initially excited

electron dissipates its kinetic energy by exciting other electrons from the valence band in the scintillator material into the conduction band. When these excited electrons return to the valence band, some of them generate scintillation photons, which are subsequently detected by a photomultiplier tube (PMT).[7] Figure 2.1 shows a schematic diagram of the process.

Scintillator detectors can provide current amplification in the range of $10^8$ to $10^9$, depending on the scintillator material, photomultiplier and electronic circuitry involved. The response time of a scintillator system is in the nanosecond time range (depending on scintillator material and photomultiplier used). Signal-to-noise ratios improves by more than 10% for ion currents of $10^{-18}$ to $10^{-20}$A can be obtained.[8]

Photomultipliers in scintillator detector systems suffer long term instability due to the same factors that affect electron multipliers: (1) ionization of residual gas present between the dynodes, and (2) polymerization of hydrocarbons on the dynode surfaces (present in all vacuum systems). Fortunately, in scintillator systems these factors can be minimized by placing the photomultiplier outside of the vacuum system.[9] Therefore, scintillator detector systems best meet the basic requirements for low particle flux measurements.

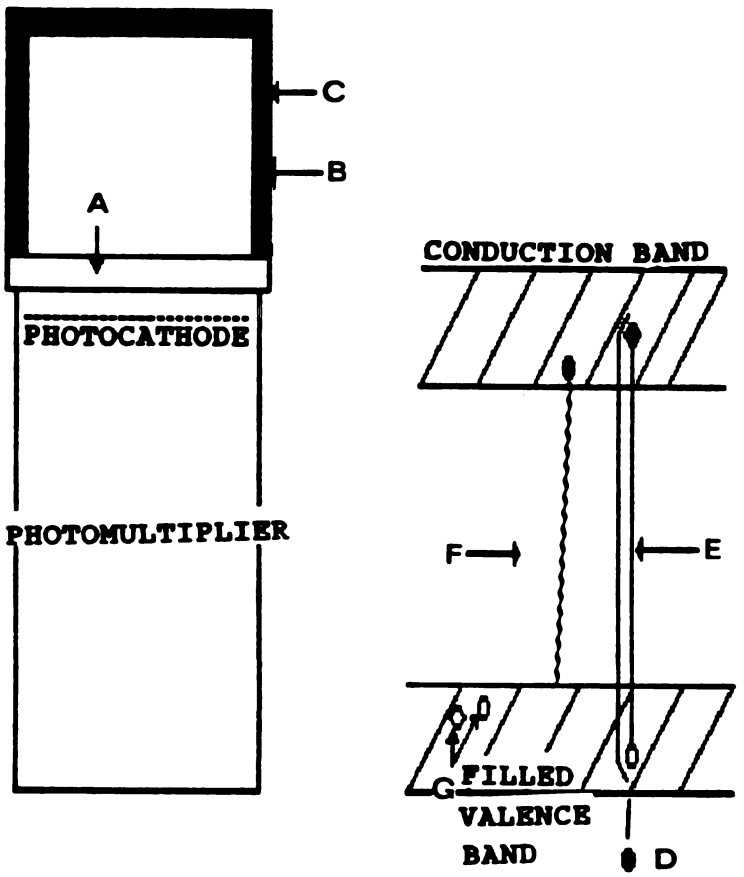


Figure 2.1. Schematic Diagram of a Scintillator detector with energy diagram (adapted from reference 7.)

A: optical coupling B: reflector ($Al_2O_3$ powder)

C: protective cover (Al) D: 30 kV electrons

E: excited electron from scintillator

F: decay of scintillator electron with emission of light G: holes

### 2.3.1 Scintillator Material Characteristics and Selection Criteria

In general, a scintillator material can be defined as a gas, a liquid or a solid in which flashes of light can occur. The two most commonly used media are liquids and solids. Liquid scintillators are used in systems in which the ionizing radiation to be detected is very low in energy and the sample to be ionized can be dissolved in the scintillator medium (e.g. radioactive materials).[10] The solid type is used with samples that cannot be dissolved in the liquid scintillator material and can be used with high as well as low ionizing radiation energy systems. In either case the number of photons produced is essentially proportional to the energy of the incident radiation. The maximum energy that can be transfered to the photo-electron is given by:

$$E_{max} = E/[1 + 1/(2\alpha)] \qquad (2.1)$$

where E = incident energy, $\alpha = E/(m_o c^2)$, $m_o$ = mass of the electron at rest and c = speed of light.[10]

In order for a scintillator material be useful it must meet certain requirements [7,8]: (1) optimized scintillation efficiency (measurement of its ability to convert absorbed radiation to detectable light), (2) wide emission spectrum with a maximum near the maximum of the spectral response of photomultiplier, (3) fast decay time, and (4) high collection efficiency. High collection efficiencies can be achieved by: (1) appropriate selection of the shape and size of the

scintillator to match the photocathode of the photomultiplier, (2) coating the surfaces of the scintillator (except the one facing the PMT) with a reflective material for the wavelength of the photons emitted, (3) appropriate match in refractive indices between scintillator, PMT and the medium between them to avoid internal reflections, and (4) appropriate thickness and diameter selection of the scintillator.

### 2.3.2 Photomultiplier Selection Criteria

The photomultiplier tube used in a scintillator detection system must have certain characteristics: (1) photocathode diameter which matches scintillator material diameter, (2) emission from the photocathode at a given wavelength (no variation in the quantum efficiency as a function of the position of the photocathode), (3) high photocathode sensitivity to blue and near-ultraviolet wavelengths, (4) good stability (no or little shift in gain with long term use), (5) low dark current (1 to 2 nAmp), and (6) fast response time (1 to 3 nsec). [11,12]

## 2.4 Design

The design of the scintillator system can be divided into two sections: (1) simulation of the ion optics transmission system by the implementation of SIMION 4.0 [3] and (2) physical space constraint considerations.

### 2.4.1 Model Systems

Modeling of various scintillator systems has been done by the use of the microcomputer program SIMION 4.0. This program simulates ion trajectories through an electrostatic field using an interactive over-relaxation method. The over-relaxation method is used to calculate the electrical potential at up to 16,000 (grid) points in the electrostatic field. This interactive program allows the user to design the geometric arrangement of electrodes, as well as to introduce: (1) voltages for the electrodes, (2) initial ion masses and velocity directions and (3) relative positions of the ions in the field.

The scintillation-type detector systems simulated with SIMION 4.0 are the ones presented by: (1) Strausser (1970),[13] (2) Daly, McCormick and Powell (1968),[2] and (3) Daly (1960).[9] These systems are designed to respond only to ions whose energies lie within a pre-selected range. The basic principle involved is that the scintillator, which is coated with a thin film of metal, responds to high energy electrons that can penetrate the coating. A single ion striking the target, an enhancer conversion dynode, causes the release of several secondary electrons which in turn will penetrate the metal coating of the scintillator and produce photons which are measured by a photomultiplier tube situated outside of the vacuum system. The number of electrons emitted per ion will depend not only on the voltage applied to the dynode but also on the type of material used in its construction. For example, if an ion strikes the surface of an enhancer

dynode made of aluminum which is at -30 keV, the number of electrons emitted by the dynode will be approximately 7 electrons per ion, whereas if the dynode is made of stainless steel only 5 electrons per ion are emitted[14].

The first modeled system (Strausser type) included an evacuable envelope containing a secondary emitter target electrode structure having a bore of conical shape (enhancer dynode). The inside surface of the bore was bombarded by the ions to be detected; the secondary electrons emitted by the dynode were focused onto a scintillator facing the exit end of the bore to give the optical photon output which was transmitted through the window to a photomultiplier.[13] Figure 2.2 shows a schematic diagram of the system and Figure 2.3 presents a SIMION ion trajectory calculation of it.

The main advantages of the in-line arrangement of the Strausser system are the simplicity of the design as well as the low range of voltages applied to the scintillator (0.1 to 10 keV). Unfortunately, the simulation program (SIMION) has shown that over 95% of the ion trajectories will miss the enhancer dynode (see Figure 2.3). Several modifications were made to the system during the modeling process in order to improve the transmission of ions, (i.e., focusing and deflection lenses were added, the scintillator and PMT were floated), but less than a 10% improvement was accomplished.

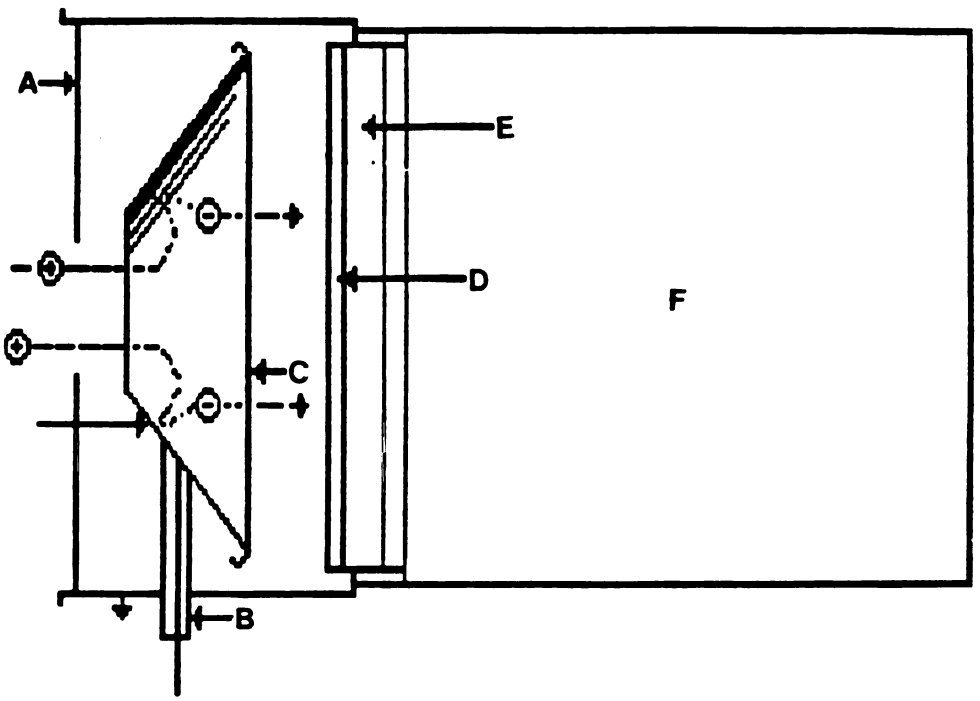


Figure 2.2. Schematic Diagram of the Strausser Scintillator-type Ion Detector (from reference 13.)

A: tubular body

B: high voltage lead and insulator

C: secondary emitter electrode

D: scintillator phosphor layer

E:transparent optical window

F: photomultiplier tube

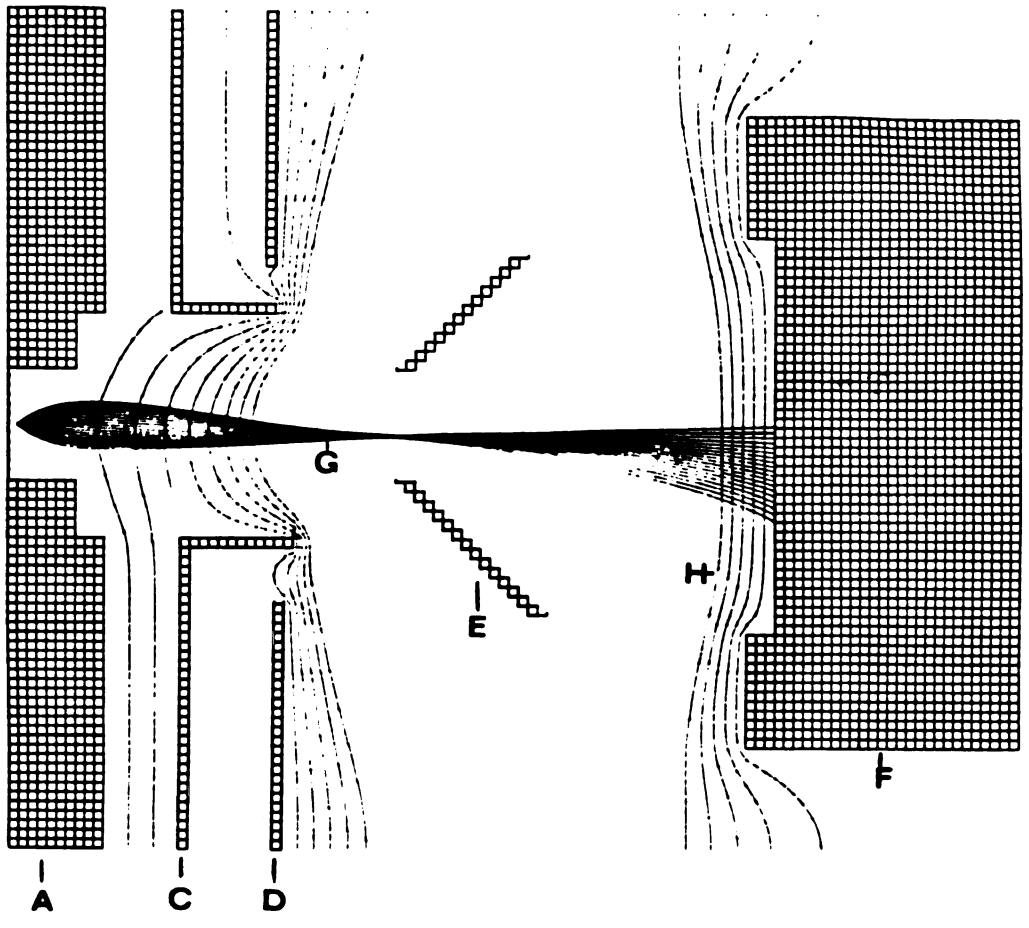


**Figure 2.3. Simion Representation of Strausser Detection System. Ion Energy is 50 eV and its Mass is 100 amu.**

**A: quadrupole = 3000V B: top deflection lens = 2000V**

**C: bottom deflection lens = 0 V**

**D: housing = 0 V E: enhancer dynode = -30 kV**

**F: photomultiplier G: ion trajectories**

**H: countour lines**

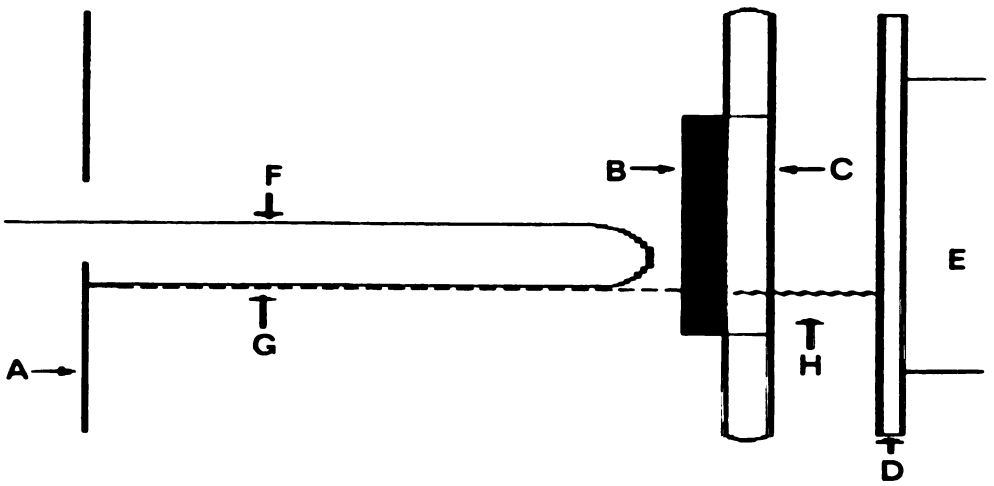


Figure 2.4. Schematic Representation of McCormick, Daly and Power Scintillator detector (from reference 2.)

A: secondary electron emitter (enhancer dynode)

B: aluminum coating C: scintillator

D: glass window E: photomultiplier

F: ions trajectory G: secondary electrons

H: light detected by photomultiplier

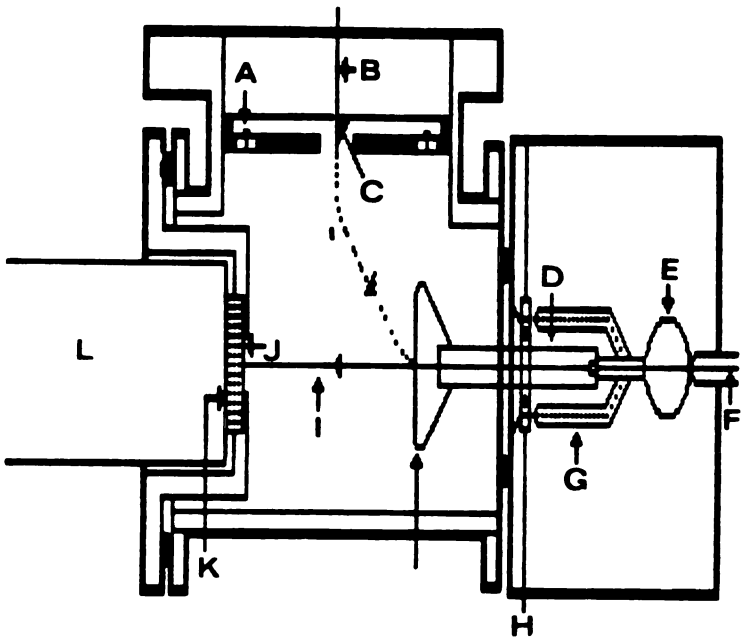


Figure 2.5. Schematic Representation of Daly Scintillation detector ( from reference 9.)

A: pumping holes

B: positive ion beam

C: ion beam entrance slit

D: stainless steel rod

E: anti corona ball

F: -40 KeV connection

G: glass metal Kovar seal

H: stainless steel with Al coating

I: secondary electron beam

J: Al coating: reflects light, conduct electrons

K: plastic scintillator

L: photomultiplier tube

The McCormick-Power-Daly system has a similar arrangement to the Strausser, except that the enhancer dynode is a flat surface and has a scintillator electrode (see Figure 2.4). The function of the scintillator electrode is to repel the ions into the enhancer, increasing the number of ions reaching the enhancer. One of the limitations of the system is that if an ion has a greater energy than the scintillator electrode it will hit the scintillator and not the enhancer dynode, thus decreasing the detection efficiency of the system.

The last system under consideration is the Daly scintillator system. In this system the enhancer dynode as well as the scintillator and PMT are at 90° to the ion trajectory (Figure 2.5).The enhancer dynode consists of aluminum, vacuum-deposited as a thin layer on a stainless steel base ground optically flat and highly polished. This increases the secondary electron yield[9] and also decreases the probability of field emission. The voltage applied to the enhancer dynode (-40 keV) assures that all of the ions entering the detector region strike the enhancer dynode, thus increasing the probability of secondary electron emission and decreasing the probability of ions reaching the scintillator. The only drawback of this system is the number of safety precautions that must be used due to the high voltage present. (For further discussion the reader is referred to references 2,6,9 and 13.)

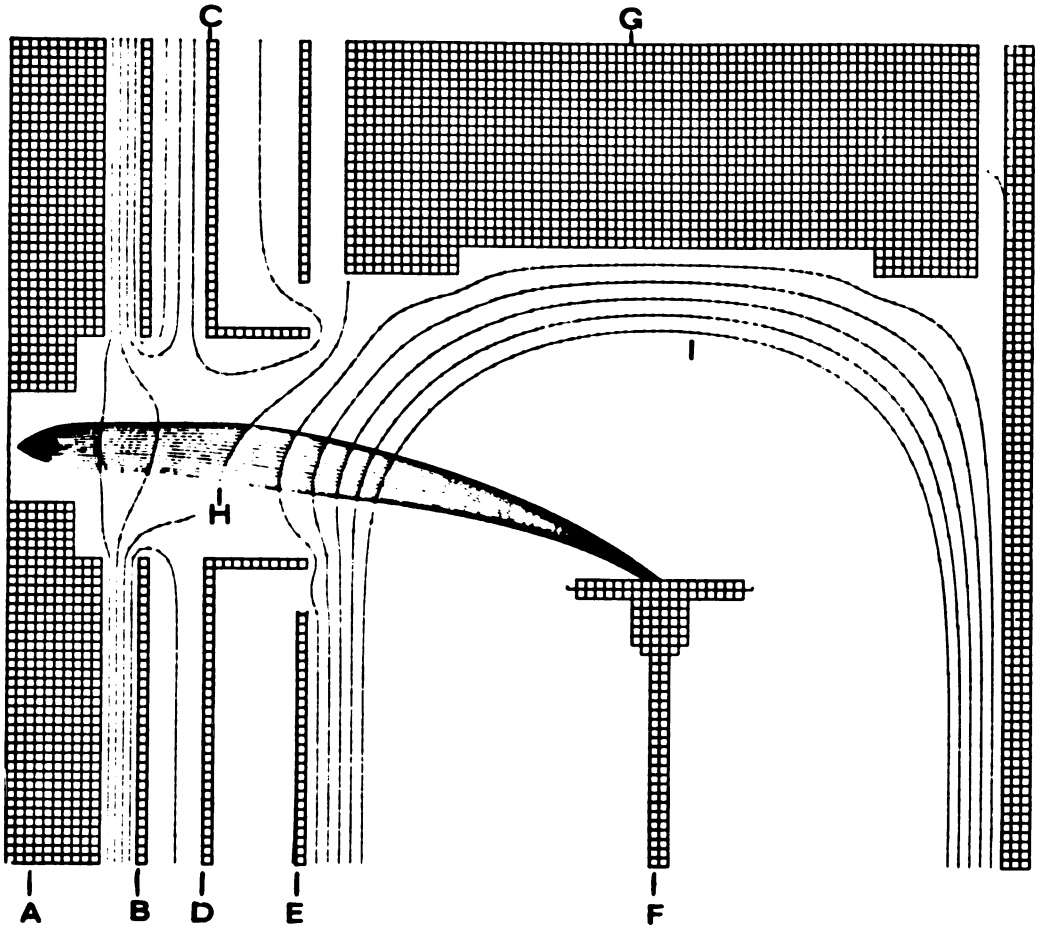


**Figure 2.6. Simion Representation of Designed Detection System.**

**Ions Energy is 50 eV and its Mass is 100 amu.**

**A: quadrupole = 3000 V  B: extractor lens = -2000V**

**C: top deflection lens = 2000 V**

**D: bottom deflection lens**

**E: housing = 0 V  F: enhancer dynode = -30 kV**

**G: photomultiplier  H: ion trajectories**

**I: countour lines**

### 2.4.2 Constructed System

The scintillator ion-type detector constructed was based on the Daly model since this system will provide the highest secondary electron emission. Several modifications were made to the initial model in order to improve transfer and transmission of the ions. Figure 2.6 presents a simulation of the trajectories of ions in this system obtained using SIMION 4.0. The system consists of: (1) transfer optics section, (2) enhancer conversion dynode, (3) scintillator and (4) photomultiplier tube.

The transfer optics section consists of: (a) an extraction lens which will be held at an electrical potential between -2000 to 100 eV to ensure the complete extraction of the ions from the quadrupole (Figure 1.1), and (2) a deflection lens to focus the ion beam to a specific area of the enhancer dynode at angle between 30° and 60° (thereby increasing secondary emission [14]). The enhancer dynode consists of an aluminum base, ground optically flat and highly polished on which aluminum is vacuum-deposited as a thin layer (to increase secondary electron emission), coupled to a -30 keV power supply (GAMA RC 10-30P) which has an output current of 0.33 mA via a 30 kV feed-thru (EFT 281 2093).

The scintillator material used (BC 408) has a decay time of 2.1 nanoseconds, and its wavelength of maximum emission is 425 nm. The light output of this material is 65% with respect to anthracene, the conventional actinometric standard. For an incident electron with an

energy of 29 keV the scintillator will emit 8 photons per incident electron.[15] The scintillator is covered with a reflective thin layer of vacuum-deposited aluminum (5000 A), which helps increase the collection efficiency of photons by the photomultiplier, which reduces damage to the scintillator from air moisture, and which provides a grounding contact surface. The scintillator is coupled to the photomultiplier tube by a thin coating film of clear epoxy (Lucite).

The photomultiplier used (R329-02 Hamamatsu) has 12 stages, a gain of $1.1 \times 10^6$, and an anode dark current of 0.7 namp at 1500 V. It has a total spread time of ≈ 7nsec; thus, its upper frequency response limit for resolved pulse operation is ≈ 140 MHz. The average charge packet for this PMT, which arrives at the anode in about a 7 nsec time interval, has an average current of $2.5 \times 10^{-5}$ A.

## 2.5 Pulse Counter

The inherent advantages of photon counting such as: (1) direct digital processing, (2) discrimination against dark current not originated at the photocathode, (3) elimination of reading error and (4) system stability against drift, have made the technique very useful in many quantitative applications.[16,17] This technique is very attractive for systems in which the radiation level is so low in intensity (where the signal-to-noise ratio approaches unity [18]) that it is difficult to obtain reliable measurements by conventional techniques (e.g., dc current, lock-in amplifier and noise

voltage).[19] The limit of detection for this technique depends on the system under consideration as well as on the required precision and accuracy.[20]

In photon counting systems the current pulses from the photomultiplier tube are usually passed across a load resistor, and the resulting voltage pulses are amplified by a fast pulse amplifier before entering a discriminator and counter. In some systems in which a high gain PMT is used the amplifier can be eliminated, and the load resistor can be connected directly to the discriminator. The final readout of the system will be affected by the counting circuitry components (RC load, amplifier and counter). The width of the pulses from the PMT or the voltage pulses in the counting circuitry results in a finite probability of pulse overlap.[21,22] For photomultiplier tubes with upper frequency responses between 70 and 200 MHz the probability of pulse overlap is assumed to be negligible.[19,23] In cases where the counting circuitry limits the frequency response (time interval between pulses or dead time, $\tau$) this may be attributed to several factors: (1) slow RC decay time with respect to its rise time, which increases the width of the peak seen by the discriminator, (2) improper discriminator reference voltage level, (3) improper selection of the counter speed.[21] Therefore, the selection of these components is critical in the performance of a photon counter system.

### 2.5.1 Design Considerations

In order to properly implement the photon counting technique several requirements must be met by the system. These requirements are: (1) high sensitivity, (2) variable sample rate control, (3) high counting stability, and (4) high count resolution. All these requirements are basically interrelated as will be seen below.

Photon counting circuits should provide a high sensitivity in order to measure signal-to-noise ratios less than unity. This can be accomplished by the appropriate selection of the: RC circuit,[21,22] discriminator level[21] and counter sensitivity (chosen to miss only 1 to 2% at an average count rate below 2 MHz).[23,24] The counter should also have a variable sample rate controller. Since the arrival rate of electrons is a random process (some of them having arrival time less than 10 nsec), by optimally adjusting the sampling rate of the counter a greater number of pulses can be detected.[22,24] In addition, the photon counting should have a high count stability in order to provide precise long time integration (greater than 10 sec), thereby reducing the noise bandwidth and allowing differentiation of individual pulses.

# CHAPTER 3

# EXPERIMENTAL APPARATUS AND OPERATIONAL PROCEDURE

The objective of this chapter is threefold: to present a description of the detection system constructed for the MSU beam instrument, to document the experimental conditions under which the detection system is operated, and to discuses the experimental problems encountered during this work, many of which were due to the author's lack of experience. The following discussion will help future users solve some of the problems that could occur again.

## 3.1 Detector Chamber

The detection vacuum chamber, shown schematically in Figure 3.1, consists of an aluminum box with outside dimensions 21.5 inches long x 11.5 inches wide x 9 inches high and 0.75 inch thick walls. The vacuum system coupled to the chamber consists of: (1) a mechanical pump, Welch Scientific Co. model R-1376, (2) a Varian 2 inch diffusion pump model HS2, which has a pumping speed of 285 l/sec, and (3) a Varian cryotrap model NRC 325, filled with methanol as refrigerant liquid. The function of the cryotrap is to minimize the amount of oil reaching the chamber from the diffusion pump. The speed of the diffusion pump is reduced to 125 l/sec due to the presence of the cryotrap. An extension flange 7 inches long x 5 inches diameter is coupled to the chamber in order to fit the quadrupole mass filter contained in the main chamber with an ion source and a leak valve

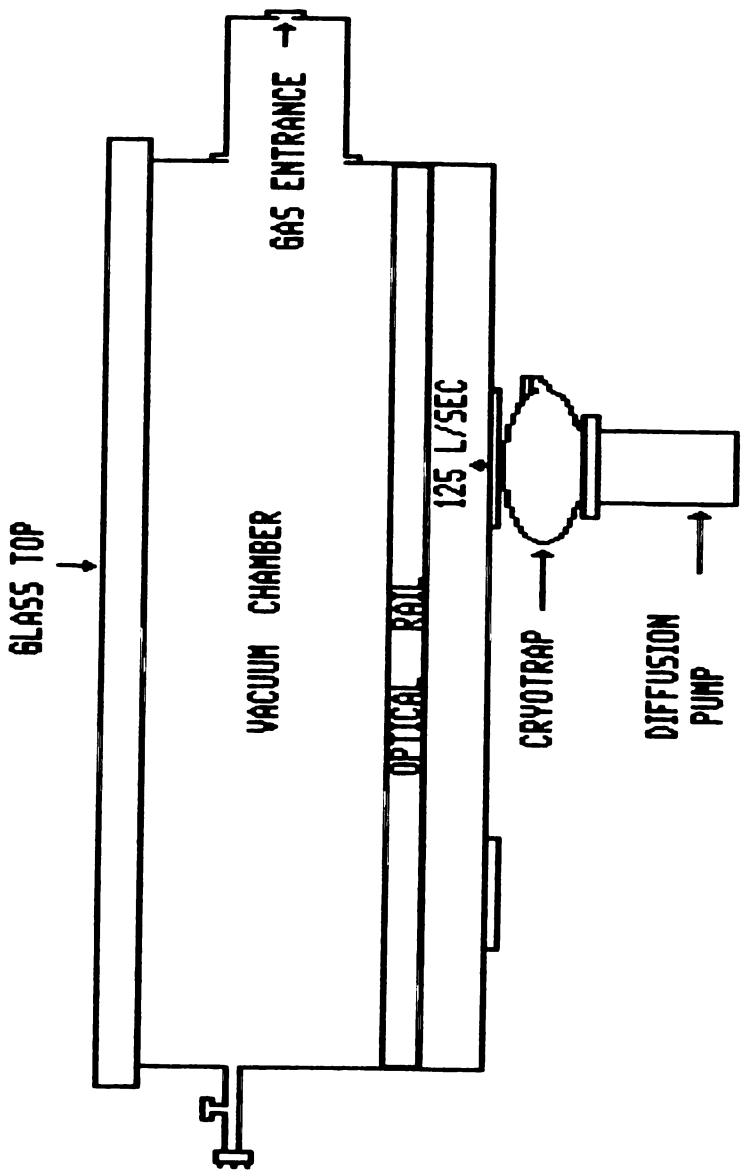


Figure 3.1. Schematic Representation of Detection System Chamber.

located at the entrance of the ion source.

The pressure inside the chamber is monitored with an ion gauge tube series 260 and an ion gauge controller model 274005 from Granville-Phillips: the transducer is located in an extension tube at the opposite end of the chamber (with respect to the ion source).

### 3.2 Mass Spectrometer and Ion Optics

The reactant gas is introduced directly into the ion source through a leak valve. The ion source is powered by a Harrison Lab. Inc., power supply (model 868A). The ions formed are guided from the ion source and focused into the quadrupole mass filter with four electrostatic aperture lenses. These lenses were supplied with the Extranuclear quadrupole mass filter (model 324-9). The dimensions of the mass filter rods are 1.9 cm diameter x 22 cm long. The lens system is powered by an Acopian ± 120 V power supply model 120J05D, while the mass filter is powered by Extranuclear power supply model 311, equipped with a high-Q head model E (mass range 0-200 amu). The ion source, lens system and quadrupole are mounted on an optical rail and are easily moved several inches in a direction parallel to the quadrupole axis. This allows the user to make any modifications in the system more easily (e.g., to move system components or to isolate different components).

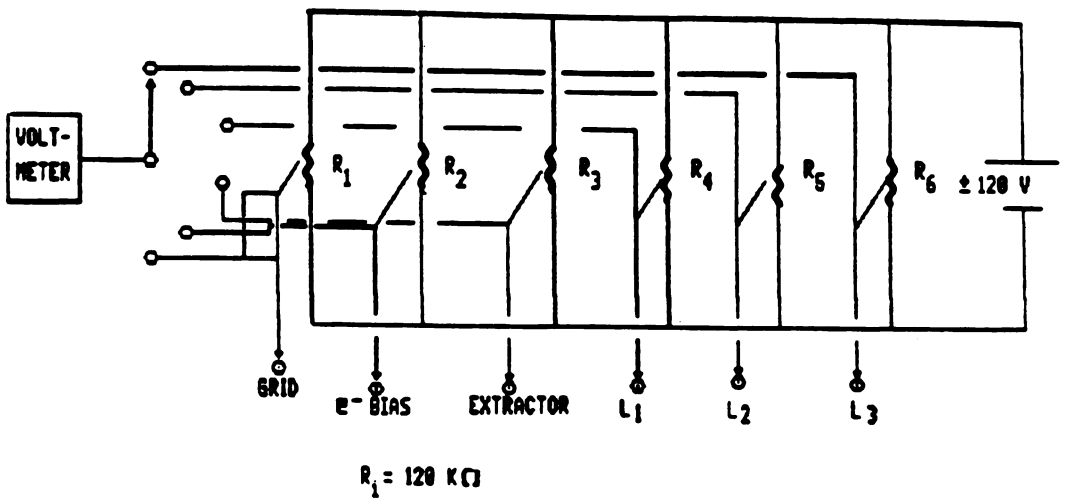


(a)

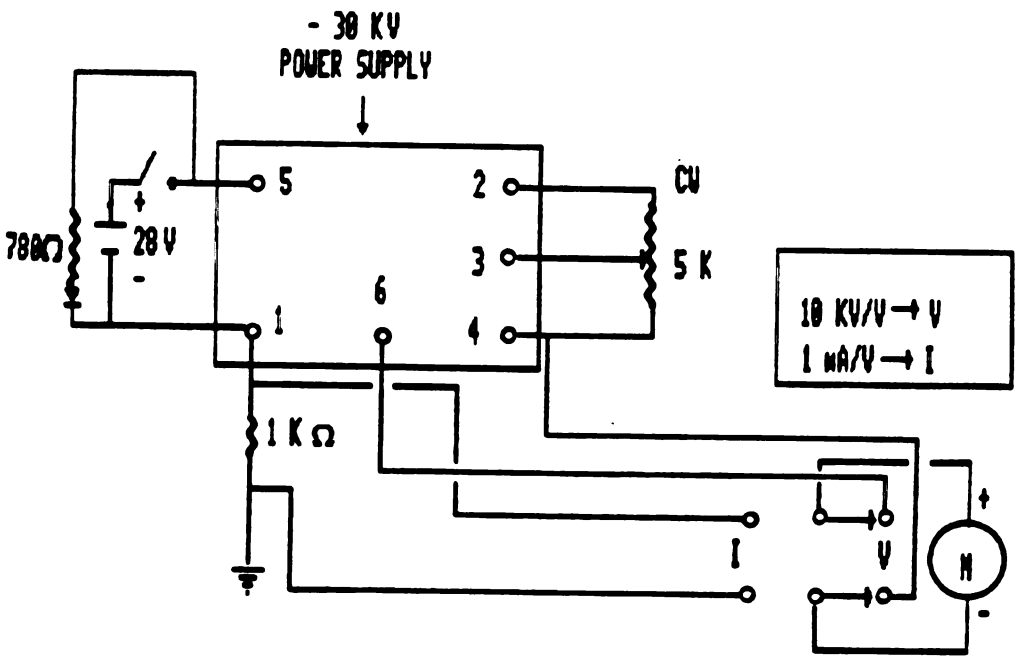


(b)

**Figure 3.2. Schematic Representation of: (a) Lens Controller Voltage Divider, (b) 30 kV Power Supply Regulator Control System.**

The voltages applied to the lens system are controlled by a home-made voltage divider (Figure 3.2a). The m/z values of the transmitted ions from the quadrupole is controlled by a dial on the front panel of the quadrupole power supply or by a frequency applied to a connector in the back of the quadrupole power supply. The detailed procedures are listed in the Extranuclear quadrupole mass filter manual.

### 3.3 Detection System

The detection system consists of: (1) two electrostatic aperture lenses (extractor and deflection lenses), (2) a housing, (3) an enhancer (or conversion) dynode, (4) a scintillator, (5) a photomultiplier, and (6) photon counting electronic circuitry (Figure 3.3).

The extraction and focusing lens is 2 15/16 inches in diameter x 0.017 inches thick and has an aperture of 1 inch. The objective of this lens is to extract the ions from the quadrupole and to focus them into the center of the deflection lens. The deflection lens is 2 15/16 inches in diameter x 0.035 inches thick; it has an aperture of 1 in., and an extension tube 1 cm long which couples the lens to the detector housing entrance. This lens is divided into two sections in order that a different voltage can be applied to each section and thereby provide more control for the deflection of the ion beam. The separation between the sections is 1/8 of an inch. In order to test

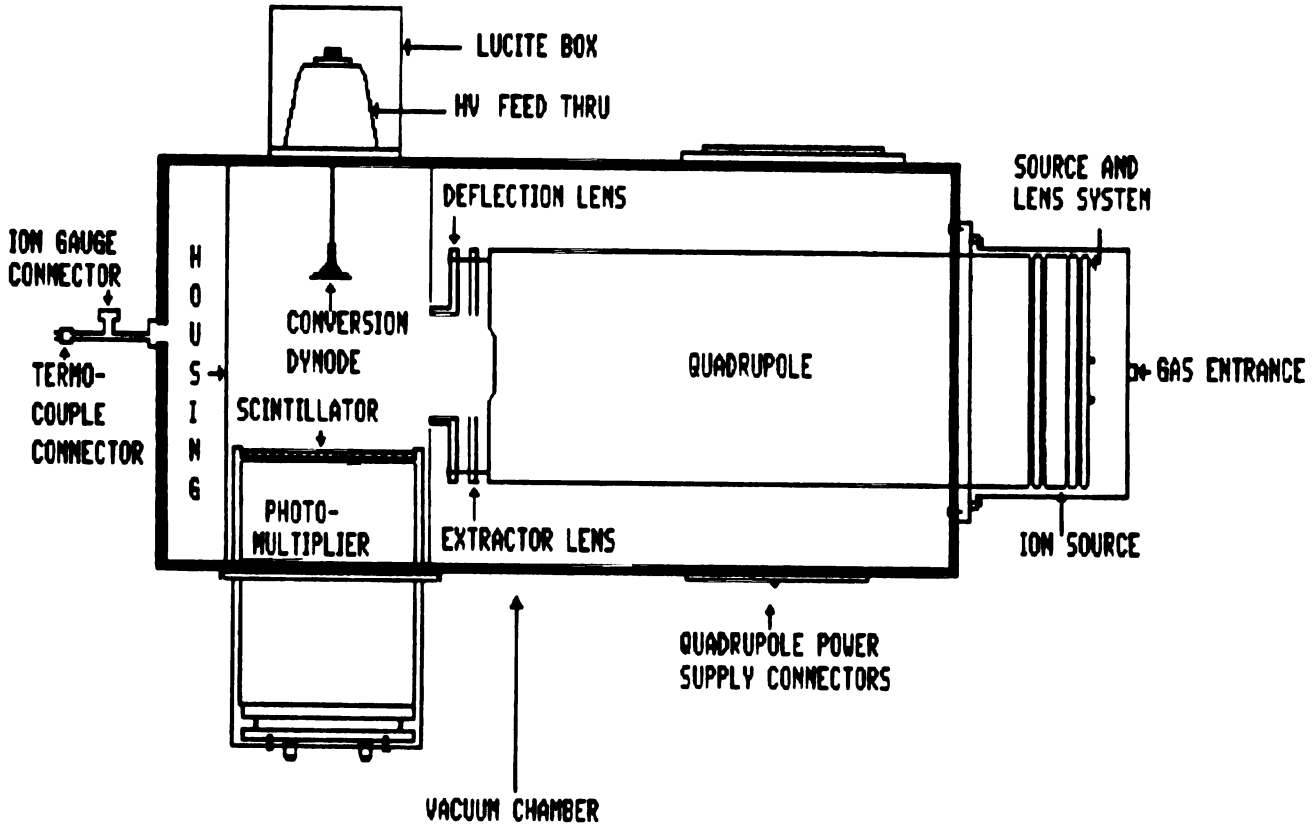


**Schematic Representation of the Detector System.**

the system, one section is kept grounded while different voltages are applied to the other section via a high voltage feedthru coupled to a flange located on the right side of the chamber.

The deflection lens ends at the entrance of the detector system housing. The entrance aperture for the detector system is 1 1/8 inches in diameter. A housing was designed to serve two purposes: (1) to constrain the high voltage applied to the conversion dynode into a specific area, and (2) to minimize the amount of light not originating from the plastic scintillator that can reach the photocathode. Located inside the housing is the conversion dynode, the scintillator and the photomultiplier tube. The housing is made of a brass tube with 3 1/4 inch O.D.and 1/16 inch wall thickness. It is placed 3/16 inch from the chamber wall.

The conversion dynode is made of aluminum and is coated with $10^4$ A of aluminum oxide. This material was selected based on its weight (a light metal is needed in order to be supported firmly by the high voltage feethru connector) and its secondary electron emission properties at the voltages of interest (Al has a ratio of secondary to primary current of approximately 7).[14] The size of the conversion dynode is 1 cm diameter x 1 cm long and is shaped like a door knob. It is connected to an external GAMMA -30 KeV power supply via a high voltage feethru. The high voltage power supply is regulated by a home-made controller system (Figure 3.2b). The control system allows the

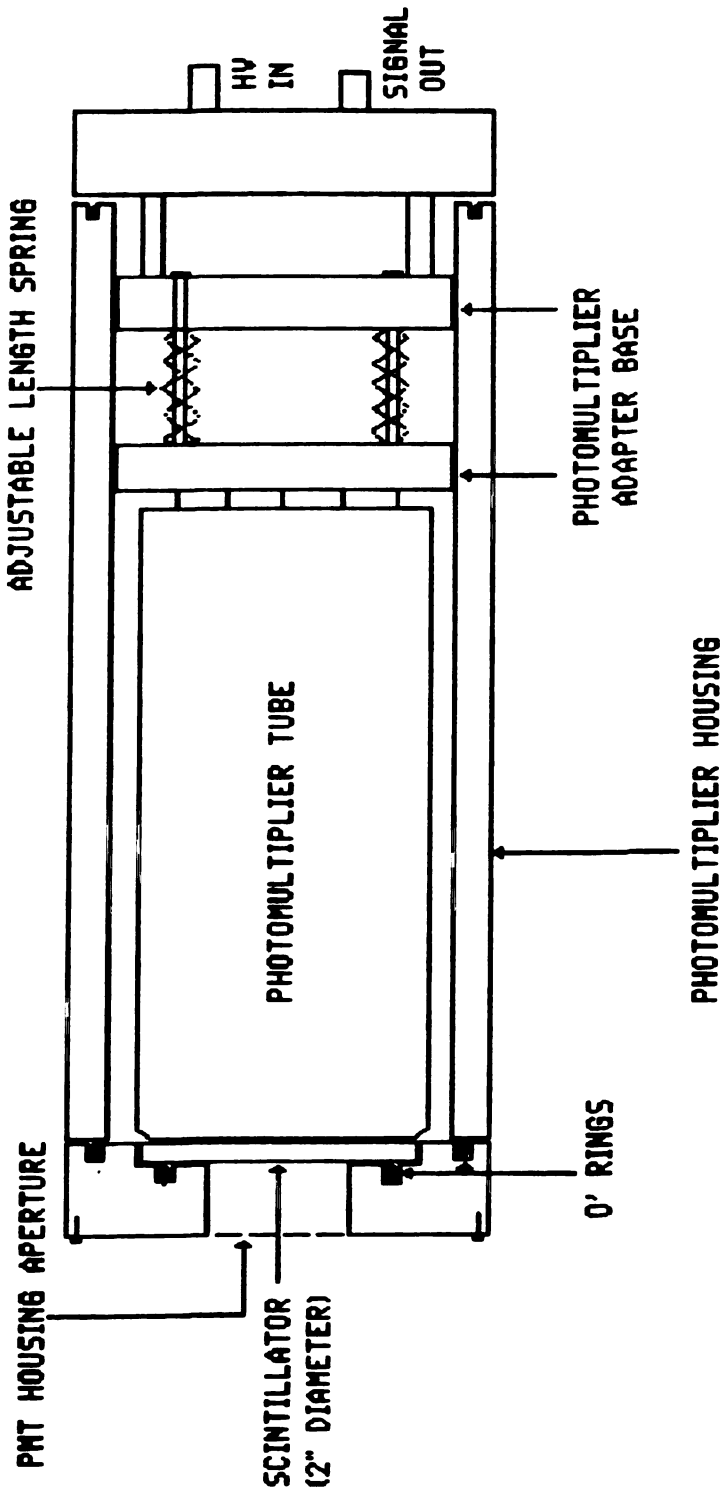


**Schematic Representation of Photomultiplier Tube Housing with Scintillator.**

operator to monitor, via a Fluke multimeter, the voltage, applied to the conversion dynode (the reading of the meter should be of 1 V for every 10 kV applied to the conversion dynode). The organic plastic scintillator and the photomultiplier tube are located across from the enhancer dynode inside of a stainless steel housing.

The photomultiplier tube is mechanically coupled to the organic plastic scintillator by the pressure that a set of springs in the PMT base exerts on the photomultiplier (Figure 3.4). The use of this configuration offers certain advantages: (1) it allows the system to be tested without the need of a coupling medium (epoxy or silicon oil used to avoid the reflection of light due to differences in refractive index between the photomultiplier and the scintillator); (2) it provides isolation from external rf fields; (3) the photomultiplier tube will have a longer life (since it is not under vacuum); (4) facile changes of photomultiplier tubes without perturbing the chamber experimental conditions can be made.

### 3.3.1 Photomultiplier Electronic Circuit

There are two ways in which the photomultiplier tube can be arranged for pulse counting: (1) the photocathode at a high negative voltage and the anode at ground, or (2) the photocathode at ground and the anode at high positive voltage. Both arrangements have their advantages and limitations. The advantage of having the photocathode

at a high negative voltage and the anode at ground is that it is easier to process the signal, since no coupling capacitor is needed. The limitation of this arrangement is the presence of high levels of dark noise that can affect low signal currents. The second circuit arrangement (anode high potential at +HV) offers the advantages of low dark current levels from the PMT and low steady-state DC levels induced by ambient light levels.[25] It is also more easily coupled to a plastic scintillator that is at ground potential. Its limitation is that the signal is difficult to process since a coupling capacitor is required in order to separate the signal from the applied voltage.[12] The coupling capacitor should have good stability.

Based on the advantages previously mentioned, the photomultiplier configuration selected for the detector system was that with the anode at a high potential, +HV. The specifications of the various components (resistors, capacitors etc.) were selected based on the ratios suggested by Hamamatsu.[27] The value of the gain resistor, $R_G$ (between the high voltage source and voltage divider) was chosen based on two factors: (1) the stability of the photomultiplier tube (for good phototube stability, the voltage divider current should be equal to or greater than 50 times the average value of the phototube current), and (2) the fact that the value of $R_G$ should be less than or equal to one half the voltage divider resistance ($R_D$).

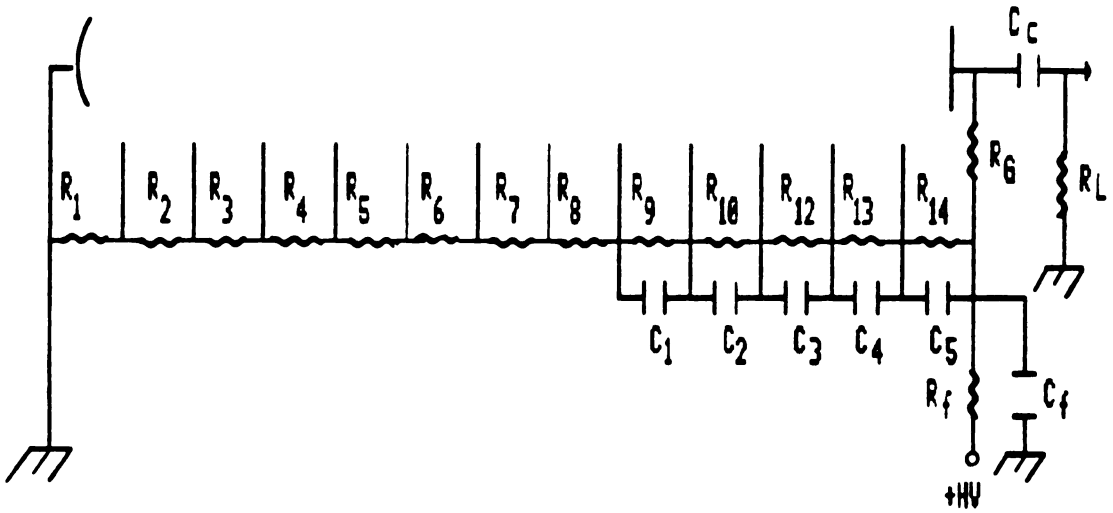


**Figure 3.5. Schematic Diagram of the Photomultiplier Electronic Circuit.**

**$R_1$=2.2 MΩ, $R_2$=$R_4$=$R_5$=···=$R_9$=470 KΩ,**

**$R_3$=$R_{10}$= 750 KΩ, $R_{11}$=$R_{13}$= 920 KΩ, $R_{12}$=1.5 MΩ,**

**$R_f$=2 KΩ, $R_c$=470 KΩ, $R_1$=6 KΩ, $C_1$= 0.02 μF,**

**$C_2$= 0.047 μF, $C_3$= 0.1 μF, $C_4$= 0.22 μF,**

**$C_5$= 0.47 μF, $C_c$= 0.001 μF, $C_f$= 0.005 μF.**

For the ratios for the resistors suggested by Hamamatsu[27] the values for the individual components in the voltage divider were determined (see Figure 3.5). The value obtained for the voltage divider resistance was 8.49 x $10^6$ ohms and the maximum value for the gain resistor $R_G$ was 4.3 MΩ. The exact value of the gain resistance can be determined based on the desired voltage drop across it. For most phototubes a voltage drop of 100 V across $R_G$ changes the gainapproximately by a factor of 2; this change in gain is sufficient to maintain a good linear operating voltage range for the phototube. Since the gain of the photomultiplier is one of the criteria used in the selection of the photon counting systems, the value of $R_G$ was chosen to keep the change in gain with the change in the PMT voltage as small as possible. Therefore, the value of the gain resistor was selected such that the change in gain obtained was less than 2 ($R_G$=470 kΩ gives a voltage drop of 79.0 volts.)

The value of the phototube resistance is given by:

$$R_{PMT} = E(\text{Applied})/I(\text{dark current}) \qquad (3.1)$$

For the R-329 phototube the dark current is 0.8 x $10^{-9}$ amp, which will yield a value of $R_{PMT}$ = 1.88 x $10^{12}$ Ω at an applied voltage of 1500V. The value of $R_{PMT} \gg R_D$, which is one of the criteria required for good stability of the electronic circuit. The stability gain is

defined as:

$$S.G. = I_D / I_P \qquad (3.2)$$

where $I_D$ is the current of the voltage divider and $I_P$ is the current of the photomultiplier. The photomultiplier current is defined[29] as:

$$I_P = [(\# \text{ counts/s})(\# \text{ p.e/keV})(V_{C.D.})(G_{PMT})]/(1 \text{ C-s-A}^{-1}/Q_{e^-}) \qquad (3.3)$$

Assuming 10,000 counts/s, 8 p.e./keV (p.e.= photoelectrons) emitted by the scintillator, the voltage applied to the conversion dynode= 30 keV/count, gain of PMT=1.1 x $10^6$, and $Q_{e^-}$= 1.6 x $10^{-19}$C/$e^-$ gives a value of $I_P$ = 4.22 x$10^{-7}$ amp. The value of $I_D$ = 1500V/(8.49 x $10^6$ + $R_G$) = 1.67 x $10^{-4}$ amp. Therefore, the stability gain is 396.6, which is a good stability value.[29]

The system has a low pass filter, consisting of a 0.005 μF capacitor and a 2 kΩ resistor, at the input of the +HV, in order to eliminate high frequency components in the signal. This filter will allow only frequencies lower than 15 kHz to pass. The coupling capacitor used in the system (selected based on the criteria of stability, voltage rating and physical size) was 0.001 μF ± 2% (3000 V).

The time constant ($\tau$) and rise time ($t_r$) can be determined using the following equations:

$$t_r = 0.35/f = (0.35)(2\pi RC) \tag{3.4}$$

$$\tau = RC \tag{3.5}$$

where $t_r$ is the rise time, R is the load or terminator resistance and C is the capacitance.[26] In the designed system the time constant as well as the rise time will be determined by the values of stray capacitance of the transmission line (30 pF/foot for RG-58/U coaxial cable), the load resistor (6 kΩ) and the terminator resistance (50 Ω). For two feet of RG-58 cable the stray capacitance will be 60 pF and a load of 6 kΩ (without a terminator resistor) the value of the time constant and rise time will be 360 and 792 nsec respectively. If a the terminator resistor is added with a value 125 or 50 Ω the time constant will decrease to 7.5 or 3 nsec and the rise time to 16.5 or 6.6 nsec, respectively. The selection criteria involved for the appropriate time constant and rise time will be discussed in the next section.

In order to test the photomultiplier as well as the linearity of the pulse electronic circuit, an LED pulsating circuit was designed

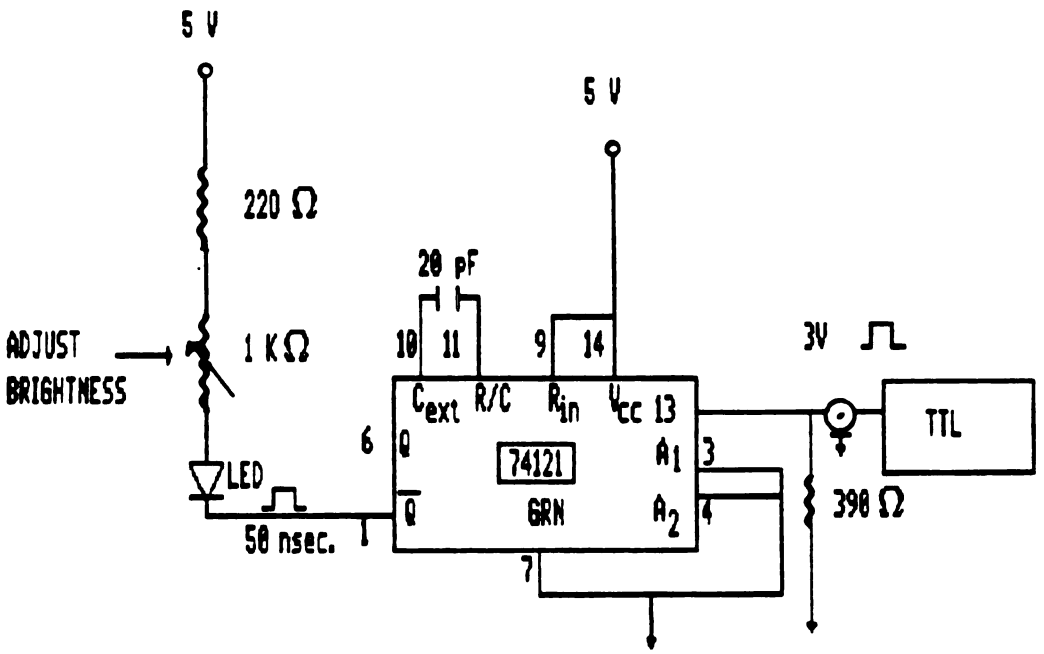


(a)

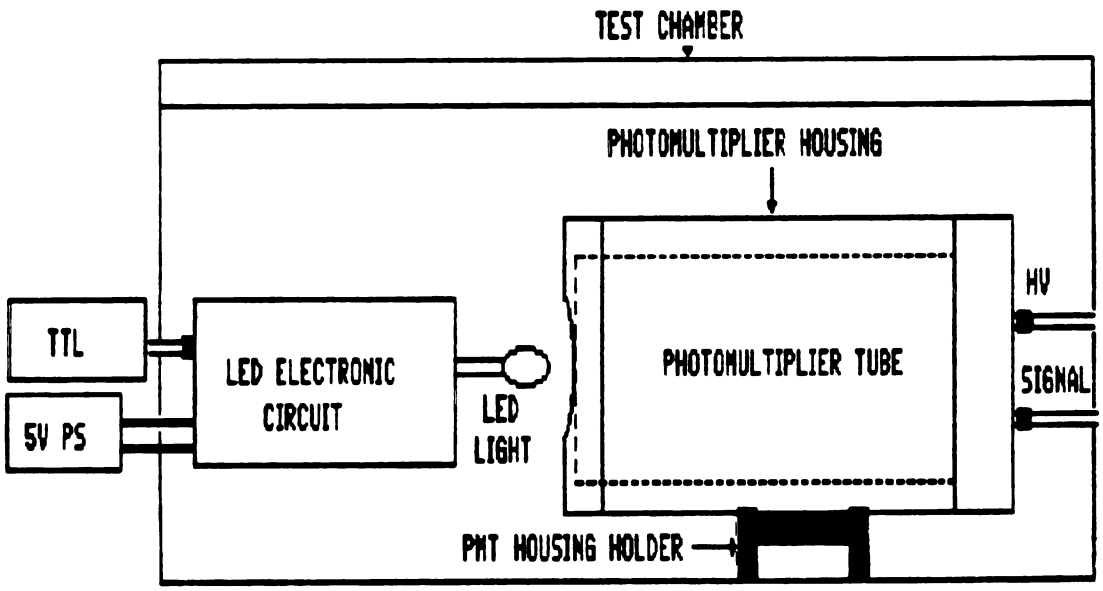


(b)

**Figure 3.6. Schematic Diagrams of: a) LED Pulsed Circuit, and b) Test System arrangement.**

(Figure 3.6 a).[28] This circuit generates a light pulse of 50 nsec and has an operating repetition rate of 1 kHz to 5 MHz.

### 3.3.2. Detector-Amplifier Interface

The output current pulses from the PMT are converted to voltages through the RC load. The value of the capacitance as well as the value of the coupling resistor must be kept as small as possible to maintain the high frequency response of the photomultiplier tube. The value of the total capacitance (PMT output capacitance + amplifier input capacitance + stray capacitance of the signal cable) should be about 30 to 60 pF. This can be accomplished by having a short signal cable (RG-58/U see section 3.2.1). The value of the resistor selected must be a compromise between that which provides high response frequency of the photomultiplier and amplifier and a value that maximizes the gain of the amplifier. If a 50 Ω resistor is selected in order to keep the PMT response frequency high, the amplifier cannot respond to such fast pulses and the signal will be distorted. Also, if the gain of the amplifier is not sufficiently high to amplify such a small signal, even when it has a fast frequency response, then the advantage of using a small resistor is lost since the signal cannot be measured by the subsequent circuitry.

In the experimental setup used, an input resistance of the amplifier of 125 Ω was utilized. This resistor value develops sufficient signal voltage pulses and provides a good frequency response from the photomultiplier.

### 3.3.3. Amplifier

In order to have good amplification of the pulsed signal voltages the amplifier must meet certain criteria: (1) minimum input capacitance so that the degradation of the input pulse be a minimized, (2) low noise in order to avoid induction of noise in the subsequent electronic components, (3) stable gain, and (4) low output impedance so that the load can be driven at high frequency.

The amplifier used in this work is an Ortec linear amplifier model 410. This amplifier has a constant input impedance of 125 Ω and an output impedance of 1 Ω that can be shunted on the input BNC connector with terminator resistance to achieve 93 or 50 Ω. It also provides a total stable gain factor in an RC shaping mode between 0.35 to 480.

It has a rise time of 80 nsec and an RC pulse shaping with time constants from 0.1 to 10 μsec ± 2%. The maximum amplifier band pass is within 3 db from 700 Hz to 4.3 MHz. The amplifier equivalent noise is less than 7 μV(rms) at the maximum gain, and its nonlinearity is

less than 0.1% from 200 mV to 10V.[30]

### 3.3.4. Pulse Height Discriminator and Counter.

Pulse signals with intensities of less than 50 mV must be amplified in order to be shaped by the discriminator and registered by the counter. In order to increase the intensity of the signal an Ortec linear amplifier model 410 was used (described in a previous section). The discriminator used in this system is an Ortec constant fraction discriminator model 463. This model allows the user to select between various types of scintillator detectors from its front panel and has a minimum discriminator setting voltage of 50mV[31] ( any signal below that voltage will not be seen). The selection of the discriminator level is done via a timing single channel analyzer, E&G&G Ortec model 420,[32] which is coupled to the linear amplifier output and the counter input (see chapter 4 for further discussion). By selecting the appropriate discriminator level the number of background signals reaching the counter can be minimized.

The final stage of the detector system is the counter. The counter used during these experiments was a Hewlett-Packard model 5216A. This counter makes frequency, period, ratios and time interval measurements.

Its sensitivity can be set between 0.1 and 10 V. It can operate over a frequency range from 3 Hz to 12.5 MHz and to 1 MHz in the Period

setting. The range interval of time measurements is from 10 μsec to 10 sec. For further details on the counter the reader is referred to the counter manual.[33]

# CHAPTER 4

# RESULTS AND DISCUSSION

## 4.1. Characterization of the Photomultiplier Electronic Circuit

In order to test the photomultiplier electronic circuit, a pulsating LED circuit was built (see Figure 3.6a), which generates a 50 nsec pulse of light. The test was conducted inside a black wooden box. The first circuit utilized had a gain resistor of 470 kΩ and a decoupling capacitor of 0.004 μf (see figure 3.5). The pulse frequencies applied to the LED circuit ranged from 1 kHz to 5 MHz. The length of the transmission cable used to couple the signal from the output of the photomultiplier to the oscilloscope was 3 ft.

### 4.1.1. Anode Response Time

The response of the PMT electronic circuit is presented in Figure 4.1. The rise and decay time of the anode under the given conditions were 0.035 μsec and 0.04 μsec respectively. The signal full-width at half-maximum was 0.05 μsec. In Figure 4.1 the presence of a small shoulder on the sides of the signal rise and decay can be observed. No explanation could be given at that time due to the lack of a better resolution oscilloscope (a 100 MHz scope was used in these experiments). Later with the aid of a 300 MHz oscilloscope and by turning on only the LED pulsating system, it was determined that the shoulders originated from the LED electronic circuit and were coupled

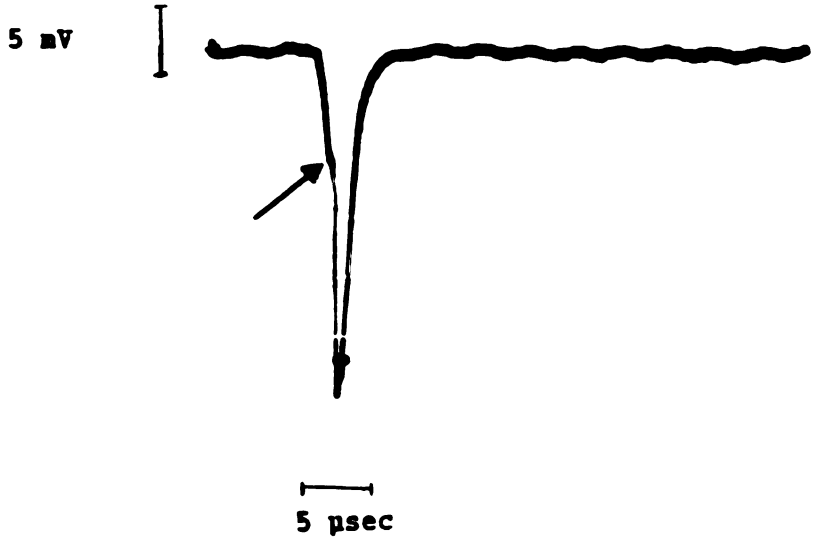


Figure 4.1. Anode Response to LED Pulsating Circuit. Applied frequency = 5 kHz; PMT applied voltage= 1500 V; Oscilloscope set at 5 µsec/div and 5 mV/div. Intensity of the peak = 19 mV, FWHM =0.9 µsec.

to the transmission cable. Several approaches were taken in order to try to solve the problem. Among them were: (a) increasing the separation between the LED and the photomultiplier, (b) adding an extra external ground at the different input and output BNC cables and connectors, (c) enclosing the LED electronic circuit inside of a grounded aluminum foil cover, (d) changing the frequency generator, and (d) rebuilding the LED electronic circuit with new components after testing each one. Unfortunately none of these steps eliminated the problem.

In order to determine the effect of the low pass filter on the anode rise time this component was eliminated. It was observed that the anode rise time had some improvement, in the microsecond range, but the resolution of the scope did not allow the quantification of such improvement. This improvement was attributed to the disappearance of the shoulder observed previously. No explanation could be found for the fact that in the presence of the low pass filter noise originating in the LED circuit could be coupled to the system. Since an improvement of the signal was observed this circuit was used to test the lens system that was employed to focus the ions onto the enhancer dynode and to test also the enhancer dynode and the plastic scintillator. This electronic circuit was later modified for reasons that would be discussed later.

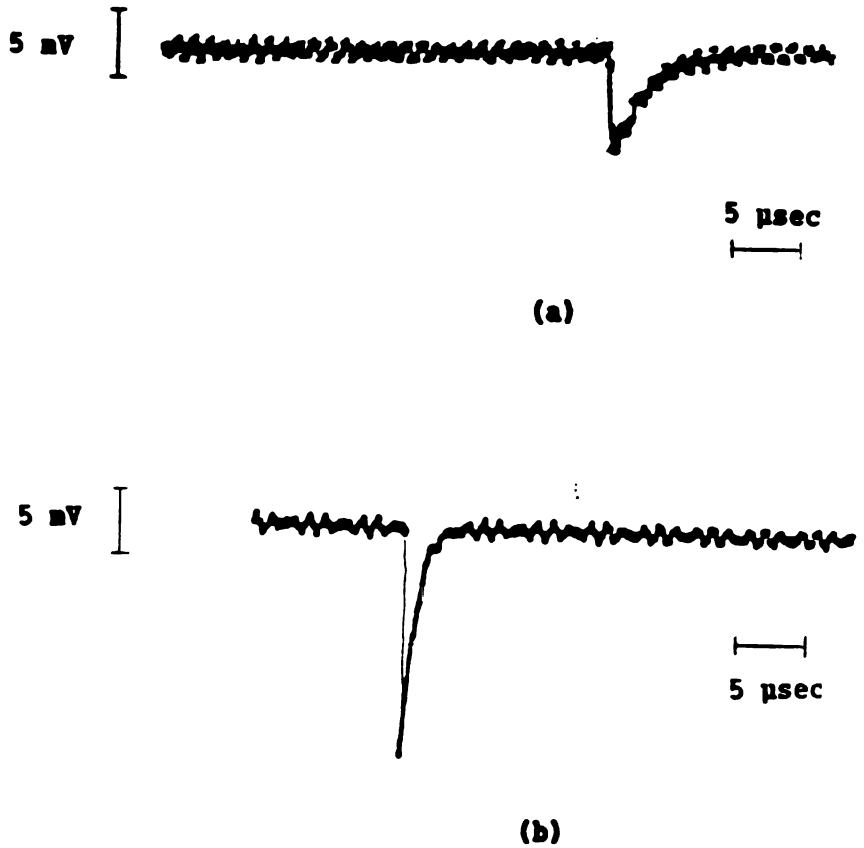


**Figure 4.2. Effect of the Length of Transmission Cable on Anode Output Signal: (a) with a 3 ft cable and (b) with a 1 ft cable. Oscilloscope set at 5 μsec/div and 5 mV/div.**

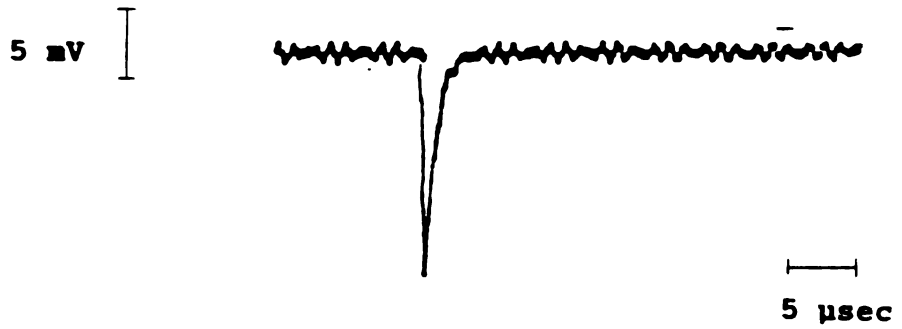


(a)

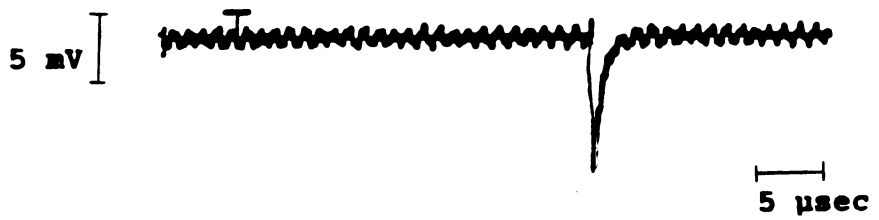


(b)

**Figure 4.3. Effect of the Value of the Terminator Resistor on the Anode Output Signal: (a) 5.8 kΩ and (b) 50 Ω. Oscilloscope set at 5 µsec/div and 5 mV/div.**

The newly modifying PMT electronic circuit again utilized the low pass filter and included a new decoupling capacitor ( 0.001 μf). This capacitor was used in order to determine the effect of the decoupling capacitor on the anode rise time. No improvement in the anode rise time was observed. Therefore the value of the decoupling capacitance does not limit the anode rise time. Improvement in the anode rise time was found when the length of the transmission cable was changed from 3 ft to 1 ft and terminated in a 50 Ω resistor. Figure 4.2 (a) and (b) shows the effect of the length of the transmission cable on the output signal of the anode while Figure 4.3 (a) and (b) shows the effect of the terminator resistor on the anode output signal. From figure 4.2 it can be observed that the output signal broadens and decreases as the length of the transmission cable is increased. In the other situation where the value of the terminator resistor is increased an increase in the signal intensity is observed but also a broadening of the signal (Figure 4.3).

### 4.1.2. Signal-to-Noise Ratio

The signal-to-noise ratio will determine if the detection system under consideration will be useful for the ion beam instrument, for which the signal intensities from the PMT are expected to be in the mV range. Therefore, the higher the value of the signal-to-noise ratio, (1000 or more), the greater the probability of detecting the scintillation signal.

The value of the signal-to-noise ratio was determined as follows: (1) the photomultiplier tube was powered at an specific voltage for a three hour period in the dark, (2) the anode signal was coupled to a counter, (3) the counter was set to its maximum sensitivity (0.01 V) and the maximum counter time (10 s), and (4) after the counter was left to stabilize for a time period of 20 minutes the number of dark counts was recorded. The same procedure was used to determine the number of counts when the LED was operated at 1.5 kHz. Table 4.1 presents the average values for the number of counts registered under the stated conditions.

The error in the number counted is given by[34] :

$$E_s = (R_s + R_b)^{1/2} \qquad (4.1)$$

where $E_s$ is the error in the signal count, $R_s$ is the signal count rate, $R_b$ is the background count rate and if T is the observation time for both the background and signal counting the signal-to-noise ratio can be expressed as:

$$S/N = (R_s^{1/2}T^{1/2})/(1 + 2R_b/R_s)^{1/2} \qquad (4.2)$$

If the background count rate is small with respect to the signal count rate this equation reduces to:

$$S/N = R_s^{1/2}T^{1/2} \qquad (4.3)$$

As shown in Table 4.1, the background count rate is much smaller than

**Table 4.1**

**Characterization of Photomultiplier Signal Count Rate**

| PMT voltage (V) | Dark Counts (counts/sec) x $10^{-3}$ | Signal Counts (counts/sec) x $10^{-3}$ | Error ($E_s$) x $10^{-1}s^{\frac{1}{2}}$ | S/N |
|---|---|---|---|---|
| 1000 | 0.0000 | 1.4396 | 3.7942 | 119.98 |
| 1100 | 0.0000 | 1.4389 | 3.7933 | 119.95 |
| 1200 | 0.0000 | 1.4377 | 3.7917 | 119.90 |
| 1300 | 0.0004 | 1.4393 | 3.7938 | 119.97 |
| 1400 | 0.0003 | 1.4366 | 3.7907 | 119.86 |
| 1500 | 0.0003 | 1.4395 | 3.7944 | 119.98 |

LED frequency = 1.5 kHz, counter sensitivity = 0.01 V, gate time= 10 seconds.

the signal count rate; therefore the expression to be used is equation (4.3). Table 4.1 also shows that the signal-to-noise ratio is 100 for a total count rate of $10^3$ counts/sec. For the experimental conditions at 1500V PMT voltage the average photocurrent is $1.8 \times 10^{-10}$ amperes. The average dark current for a rate of 0.3 counts/sec is $5.3 \times 10^{-14}$ amperes. This represents a reduction in the value of the dark current by a factor of 1000 compared with the anode dark current reported by Hamamatsu Co., (0.8 namp).

## 4.2. Amplifier-Discriminator Signal Coupling

The output signal from the photomultiplier tube was directly coupled to the 410 linear amplifier with the amplifier output in turn coupled to the constant fraction discriminator. Amplification of the signal was necessary because the intensity of the signal from the PMT was too small for the minimum value required by the discriminator (50 mV). Two problems were encountered when the anode output signal was coupled to the amplifier and discriminator: (1) the minimum time constant of the output signal from the amplifier was 0.01 μsec, and (2) the discriminator setting control was very sensitive to any small change. The first problem (limitation on the time constant) did not allow a true reproduction of the anode output, since it broadens the signal to a value of 0.01 μsec and causes pulse overlaps. The second did not permit the setting for the correct discrimination of the number of dark count with respect to the signal. Table 4.2 presents the

**Table 4.2.**

**Count Rate as a Function of Discriminator Voltage**

| Discriminator Voltage (mV) | Dark Counts (counts/sec) x $10^{-3}$ | Signal Counts (counts/sec) x $10^{-3}$ |
|---|---|---|
| 50.040 | 9.2153 | 18.6704 |
| 50.060 | 9.3532 | 16.6708 |
| 50.080 | 1.5688 | 16.6617 |
| 50.100 | 0.3203 | 16.6516 |
| 50.120 | ------ | 16.6770 |
| 50.140 | ------ | 16.6531 |
| 50.160 | ------ | 16.6711 |
| 50.170 | ------ | ------- |

**Amplifier conditions: gain= 3, fine gain= 1.5, integration time constant = 0.1 μsec. PMT voltage = 900 V. LED frequency = 1.5 kHz.**

counts values after the signal was passed at different discriminator values. It can be observed that the number of signal counts did not change even when the discriminator voltage was set at a value which should discriminate against the dark counts. This could be attributed to some pulse overlap in the signal or to noise developed in the amplifier.

In order to try to overcome the problem a Colinear preamplifier was placed at the anode output and coupled to a single timing channel analyzer. Unfortunately, the preamplifier used had a 50 Ω input resistor and output that decreased the signal-to-noise level. The single timing channel analyzer required a minimum signal level of 100 mV that could not be met the by preamplifier signal level. The same configuration was used with the constant fraction discriminator but the same signal level obtained from the amplifier could not met the limiting input voltage of the discriminator. Since no improvement could be made in the characterization of the photomultiplier electronics and signal processing using this configuration a mass spectrometer was employed in order to try to simulate the real system conditions.

### 4.3. Mass Spectrometer Test System

The description of the system was given in the previous chapter. In order to use the ion beam from the mass spectrometer to generate the

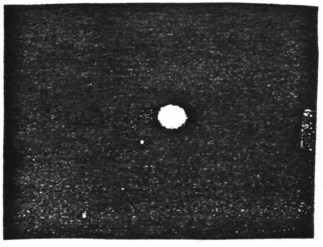

(a)

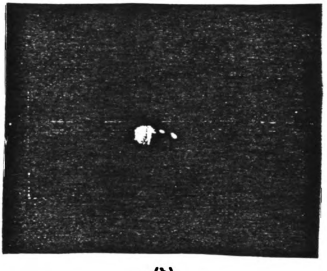

(b)

Figure 4.4. Beam Visualization of Test Background Signal in the Vacuum Chamber. Conversion dynode voltage = -30 kV. (a) Deflection lens voltage = 0 V, (b) deflection lens apply voltage = 70 V.

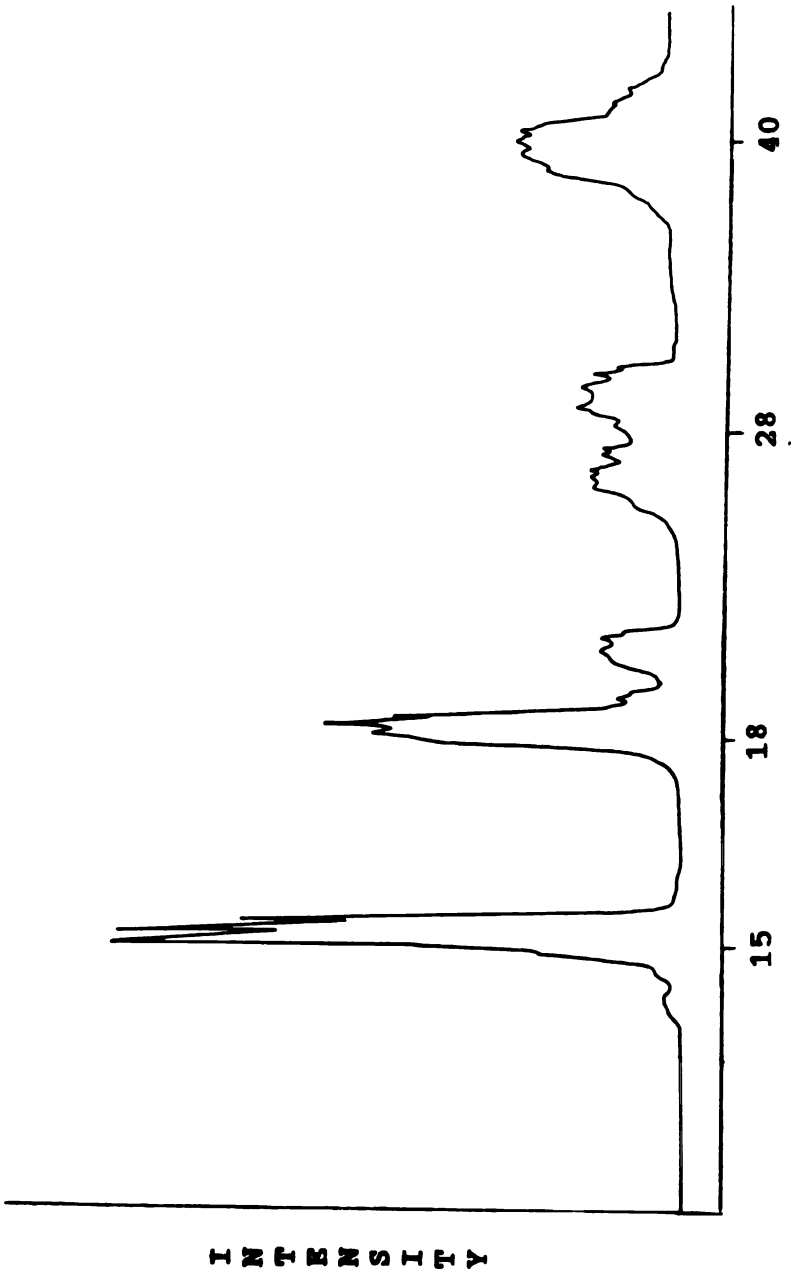


Figure 4.5. Mass Spectrum of Background Gases in the Vacuum Chamber.

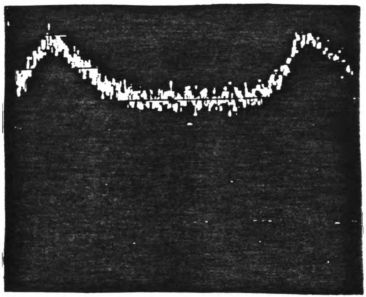

Figure 4.6. Frequency Dependent Signal from PMT Electronic Circuit without Low Pass Filter. PMT voltage = 1500 V, Conversion Dynode voltage = -30 kV.

anode output signal it was necessary to make the ions reach the conversion dynode and to observe an output signal (electrons emitted) via a Faraday plate at the position where the scintillator and photomultiplier tube was going to be placed. This experimental set-up has a threefold advantage: (1) it allows the optimization of the ions exiting from the source by adjustment of the voltages of the lenses between the source and the quadrupole; (2) one can validate and optimize voltages of extractor and deflection lenses between the quadrupole and the conversion dynode and (3) the utility of the Daly conversion dynode can be determined in the experiments.

The signal output obtained after optimizing the previously mentioned experimental arrangement was $2.0 \times 10^{-8}$ amp. at an applied conversion dynode voltage of -30 kV. It was observed that decreasing the conversion dynode voltage resulted in a decrease in the signal current was observed. This agrees with the theoretical modeling done with SIMION 4.0. In addition, a beam visualization was done using the scintillator as a visualizing screen. Figure 4.4 shows the signal image obtained during the experiments.

Figure 4.5 presents the mass spectrum of the background gases present in the chamber. After the background mass spectra were obtained the photomultiplier tube for pulse counting was placed in the chamber. The electronic circuit used initially did not contain a low


(a) 5 μsec

(b)

Figure 4.7. a) Anode Output Signal of Background Gas in the Chamber: (a) without Discriminator, and (b) with after discriminator with amplifier. Mass = 18 amu, discriminator set at 50.04 mV and amplifier at a gain of 1.

Table 4.3.

Photomultiplier Count Rates Using the Mass Spectrometer

| $PMT_{voltage}$ (V) | Dark Counts (counts/sec) x $10^{-3}$ | Signal Counts (counts/sec) x $10^{-3}$ | Error $E_a$ | S/N |
|---|---|---|---|---|
| 1500[a] | 0.0003 | 6.6002 | 77.476 | 244.98 |
| 1500[b] | 0.0402 | 608.098 | 780.31 | 2467.3 |
| 1500[c] | 0.0003 | 6.4170 | 80.106 | 253.32 |
| 1500[b] | 0.0402 | 644.566 | 802.85 | 2538.51 |

(a) monitoring $H_2O$, m/z = 18, without amplification.

(b) amplifier conditions: gain = 1, fine gain = 1.5, integration time constant = 0.1 μsec.

(c) monitoring $N_2$, m/z = 28, without amplification.

Quadrupole controller setting: high cal = 1.2, low cal = 0.75, low mass =0.3, resolution = 5, delta M = 0.

pass filter. With this electronic circuit in the system presented one problem was encountered; when the mass spectrometer was scanned and approached a region where an intense peak was present a frequency dependent signal was observed. Figure 4.6 shows the frequency component observed. This problem was attributed to the presence of rf noise on the signal output.[35] It was corrected by placing a low pass filter in the photomultiplier tube electronic circuit . Figure 4.7a shows the anode signal output and Figure 4.7b shows the output of the anode signal after passing through the constant fraction discriminator amplification. It can be seen from Figure 4.7 that the anode signal output has a greater intensity than the one generated by the LED test circuit. Table 4.3 presents the count rate of the system under consideration. The procedure used to obtain these data was the same as the one used with the LED circuit (Section 4.1.2).

For the experimental conditions employed the average charge content of the pulses changes with the applied photomultiplier voltage, thus causing a photocurrent change. The average charge content at 1500 V for the signal is $1.2 \times 10^{-9}$ amperes without amplification and with amplification is $1.1 \times 10^{-7}$ amperes. The equivalent dark current was $5.3 \times 10^{-14}$ amperes without amplifier and $7.1 \times 10^{-12}$ amperes with it.

These values represent a reduction in the dark current of the photomultiplier tube, and demonstrate the inherent advantage of the photon counting technique in systems were the signal intensity is very low.

# CHAPTER 5

# SUMMARY AND CURRENT STATUS OF THE DETECTION SYSTEM

## 5.1. Summary

The data presented in the previous chapter for two different arrangements of the photomultiplier circuitry for pulse counting indicates a fast response time (in the nanosecond range.) The exact characterization of the anode response time was not possible at the time of this work due to various factors. These include: (1) lack of a pulsed emission light source that has a pulse width of 5 nanoseconds or less, and (2) the presence of a frequency component in the anode output signal that did not allow the exact determination of the response time of the signal. Since the LED pulse circuit could not be operated at such small pulse widths and because the inclusion of a low pass filter caused an interference signal at the same frequency as the anode output signal, only an estimate of the value of the anode response signal could be made, and this is 50 nanoseconds ± 10%.

In addition to the characterization of the PMT electronic circuit, an attempt to determine the linearity of the counting system was made. Knowledge of the pulse height distribution would give information on where the discriminator can be set for the best stability and discrimination against dark counts. Unfortunately the discriminator used did not allow the proper setting for the discrimination of the

used did not allow the proper setting for the discrimination of the dark count from the anode signal response ( see Table 4.2) Although this test could not be performed properly the signal-to-noise ratio was obtained by determining the rate of dark counts and the rate of signal counts (see Table 4.1.) The dark current of the photomultiplier was observed to be lower than the value reported by Hamamatsu Co., for the PMT operating at 1500V.

These series of experiments could not provide the complete characterization of the system, nonetheless, since the PMT pulse circuitry was operating in the nanosecond range it was possible to test the rest of the detector system (extractor and deflection lens, enhancer dynode and scintillator). It was found that the SIMION modeling correctly predicted the behavior of the system. It was also observed that the intensity of the signal decreased as the voltage applied to the enhancer dynode was decreased, and that signals obtained with an operating voltage (applied to the enhancer dynode) over -15 keV did not require any type of amplification. In addition, a decrease in the dark current and a good value for the signal-to-noise ratio was observed (see Table 4.3.)

## 5.2 Current Status of the Detector System

The detector system for photon counting is at the present moment in its final stage of characterization. In order complete its

characterization a new discriminator and an amplifier or preamplifier (with a smaller time constant) will be used. This will permit the determination of the linearity of the system.

After its final characterization the system will be coupled to the ion beam instrument. At that stage experiments similar to those done with the quadrupole mass spectrometer will be performed with the entire system (determination of: dark counts, signal counts, shape of the output pulses, linearity and stability measurements). Once those experiments are finished it will be necessary to automate the system. This will allow the user to program voltages, discriminator settings and counting times via a computer system and also will facilitate the handling of the data obtained during experiments.

## REFERENCES


1. Melton, C.E.; Principles of Mass Spectrometry and Negative Ions, edited by Marcel Dekker, New York, 1970, p.141.

2. Daly, N.R.,McCormick, A., Powell, R.E.; Rev. Sci. Instr., 39, 1163, (1968).

3. Idaho National Engineering Laboratory, EG&G Idaho Inc., Idaho Falls, ID.

4. Harris, F.M., Trott, G.W., Morgan, T.G., Brenton, A.G., Kingston, E.E., Beynon, J.H.; Mass Spectrom. Rev., 3, 209, (1984).

5. Hamamatsu Corporation, Technical Manual RES-0795, Bridgewater, N.J.

6. Dietz, L.A., Hanrahan, L.R.; Rev. Sci. Instrum., 49(9), 1250, (1978).

7. Hurlbut, C.R.; Plastic Scintillators a Survey, (1985), Bicron Co., Newbury, OH.

8. Bellian, J.G., Dayton, R.R.; NaI(TL) Scintillation Detectors, Bicron Co., Newbury, OH.

9. Daly, N.R.; Rev. Sci. Instrum., 31(3), 264, (1960).

10. Burle Industries Inc.; RCA Photomultipliers Handbook, Lancaster, PA., (1980).

11. Malmstadt, H.V., Barnes, R.M., Rodriguez, P.A.; J. Chem. Educ., 41, 263, (1964).

12. Hamamatsu Corporation, Application Manual RES-0790, Bridewater, N.J.

13. Strausser, Y.E.; U.S. Patents Applications No. 3,538,328, (1970).

14. Bourne, H.C.Jr., Cloud, R.W., Trump, J.G.;J. Appl. Phys., 18, 596, (1955).

15. Vasko, B.A.; Personal Communication, Bicron Technical Sales Dept.

16. Viterbini, M., Adriani, A.; Rev. Sci. Instrum., 60(2), 280, (1989).

17. Winefordner, J.D., Vickers, T.J.; Anal. Chem., 42, 206R, (1970).

18. Nakamura, J.K., Schwartz, S.E.; Appl. Opt., 7, 1073, (1968).

19. Franklin, M.L., Horlick, G., Malmstadt.; Anal. Chem., 41, 2, (1969)

20. Rosenstock, H.M.; Int. J. Mass Spectrom. Ion Phys., 20, 139, (1976).

21. Ingle, J.D. Jr, Crouch, S.R.; Anal. Chem., 44, 777, (1972).

22. Ingle, J.D.Jr., Crouch, S.R.; Anal. Chem., 44, 785, (1972).

23. Darling, E.J.; PH.D. Thesis, Michigan State University, 1978.

24. Dietz, L.A.; Rev. Sci. Instr., 36, 1763, (1965).

25. McHose, R.C.; RCA Fast Photomultiplier Tube Technique AN-4797, PA, (1985).

26. McHose, R.E.; RCA Photodetector AN-4884, PA, (1972).

27. Hamamatsu Corporation; Photomultiplier Tubes For Scintillation Counting & High Energy Physics, pp. 26, N.J., (1985).

28. Marti Rabb; Personal Communication, Electronic Designer, M.S.U. Department of Chemistry.

29. Bicron Corporation; Application Notes SC-110, (1985), Bicron Co., Newbury, OH.

30. E&G&G Ortec Co; Instruction Manual Model 410, (1966), E&G Ortec Co., Oak Ridge, TN.

31. E&G&G Ortec Co; Instruction Manual Model 463, (1966), E&G&G Ortec Co., Oak Ridge, TN.

32. E&G&G Ortec Co; Instruction Manual Model 420, (1966), E&G&G Ortec Co., Oak Ridge, TN.

33. Hewlett Packard; Instruction Manual Electronic Counter 5216A, (1969), Hewlett Packard Co., Santa Clara, CA.

34. Norton, G.A.; Appl. Opt., 7, 1, (1968).

35. Marsh, E., Prat, L., Gilton, T., Cowin, J.P.; Rev. Sci. Instrum., 60(9), 3070, 1989.